Analysis of heat treatment on hydrogen impurities associated to Zn vacancy and other intrinsic defects in ZnO nanoparticles

V. P. Singh [a, #], M. Kumar [b, #, *], A. Kumar [c], S. Sharma [d], C. Rath [e], S. H. Park [f]
[a] *Department of Physics, United College of Engineering and Research, Prayagraj-211010, India*
[b] *Department of Electronics and Communication Engineering, Chandigarh Engineering College, Chandigarh Group of Colleges, Jhanjeri-140307, India*
[c] *Department of Physics, Christ Church College, Kanpur-208001, India*
[d] *Department of Electronics and Communication Engineering, Indian Institute of Information Technology, Prayagraj-211015, India*
[e] *School of Materials Science and Technology, Indian Institute of Technology (BHU), Varanasi-221005, India*
[f] *Department of Electronics Engineering, Yeungnam University, Gyeongsan-38541, South Korea*

This paper will present a comprehensive examination of unintentional hydrogen impurity in ZnO along with its stability and application. Results are based on the sampled synthesized by hydrothermal technique. The unique outcome of this study is co-existence of Zn and Hydrogen impurity including their complexes. Moreover, the existence and role of Zn and O di-vacancies also discussed. Synthesized nanoparticles analyzed by using XRD pattern, photoluminescence spectrum, Raman spectrum and positron annihilation experiment. The broad luminescence in visible region confirms the presence of different defects and impurities. Breakdown of the translation symmetry of the ZnO lattice also discussed based on Raman spectrum. Positron life time components provide the support to define the role of hydrogen impurity.

(Received December 19, 2024; Accepted April 1, 2025)

Keywords: Hydrogen impurity, ZnO Nanoparticles, Photoluminiscence, Positron annihilation

1. Introduction

Hydrogen impurity in ZnO material is an important point of study, which control many chemical reactions for many exciting applications such as energy generation & conversion and electrical conduction etc [1]. This impurity can be controlled by novel synthesis process and new precursors including post synthesis processing techniques [2]. To create new applications, it is crucial to manage the shapes of nanocrystallites for producing the next wave of smart and functional materials that integrate hydrogen impurities (H+/H-). The unique attributes of nanomaterials are influenced by their dimensions and form, as different facets or orientations in a crystal may display differing physical and chemical properties. Consequently, novel synthesis and processing techniques are needed to enhance the comprehension of hydrogen impurity manipulation alongside growth mechanisms. ZnO, recognized for its diverse morphologies, is a significant functional material employed in numerous applications. Due to noncentrosymmetricity, ZnO is extensively used in piezoelectric applications for surface acoustic wave (SAW) devices, especially for delay lines. In addition, the broad and distinct band gap (3.4 eV) and 60 meVexciton binding energy enables excitonic transitions at room temperature; this characteristic can be utilized in semiconductors and displays exceptional electronic (diode), optical (UV laser), and magnetic (DMS) attributes. Recent research indicates that ZnO nanostructures appear in highly organized

* Corresponding author: mkshekhawat22@gmail.com
# First and second authors are equally contributed
https://doi.org/10.15251/JOR.2025.212.217

formations [3-5]. These structures were created in regulated growth environments. Several techniques can be utilized to prepare this material. The literature comprises various accounts of high-temperature growth methods, including MOCVD, VPT and VLSE processes, vapor-phase epitaxy, and template-assisted growth [6-8]. Gas-phase methods frequently require elevated temperatures and expensive machinery. A major constraint of these growth methods for epitaxy is related to the fix substrate or integrated into a matrix. Numerous substrates, including sapphire, are both non-conductive and costly, making them inappropriate for semiconductor integration, thereby restricting more feasible and appropriate new applications of ZnO nanostructures in optical and electronic fields. Conversely, multiple lower temperature growth methods, such as chemical/solvent environment processes and electrochemical methods have been productively utilized to produce well-organized arrays of anisotropic ZnO in different shapes. Microemulsion, solvo/hydro-thermal and solution-based co-precipitation represent various recognized chemical techniques employed for the production of ZnO [11, 12]. To achieve diverse morphologies, many researchers have utilized various types of substrates (acting as seed layers) and added different substances like as ligands with organic nature in company of impurities of ionic metal. In contrast to other synthesis techniques, precipitation methods performed in unpressurized aqueous solutions offers significantly higher yields, a simpler process, and the possibility of large-scale production without requiring substrates or surfactants. Minor changes in any reaction parameters can result in notable variations in the size and arrangement of zinc oxide crystals generated from aqueous solutions. Many studies have analyzed the significant impacts that alterations in different growth conditions, like as agitation, temperature, as well as pH. These parameters greatly affect morphology of synthesized nano product. Generally, the procedure starts with the accumulation of zinc hydroxide in amorphous state, which subsequently crystallizes and experiences thermal decomposition and dehydration, leading to the development of solid ZnO nuclei. The process by which zinc hydroxide converts into zinc oxide, the factors that affect product morphology and zinc hydroxide's possible function in this transformation are still mostly unclear.

The objective of this study is to grow simplistic thoughtful experimental concepts to tune hydrogen impurity with cost-efficient and environmentally-friendly aqueous solution synthesis route for ZnO. This study also investigates the feasibility of controlling the crystal growth with changing the post heat treatment of the synthesized ZnO for the tuning of hydrogen impurities. Five calcination temperatures are used to study ZnO nanocrystallites and characterized through various techniques in respect of tuning hydrogen impurities.

2. Synthesis technique

ZnO nanoparticles in powder form were synthesized through the standard solution-based co-precipitation method. Zinc nitrate functioned as the precursor, while NaOH functioned as the precipitating agent at a defined molarity. The solution was kept at 80 °C and mixed for 30 minutes. After purifying and extensively rinsing the precipitate first with purified water and acetone, nanopowder of white color was received. The product was subsequently dried for 12 hours at a temperature of 80 degrees Celsius. A Rigaku powder diffractometer with an 18 kW rotating anode (Cu Kα) was used to perform an x-ray diffraction (XRD) analysis on the dried powder. A photoluminescence study was performed utilizing an Ocean Optics spectrometer and a pulsed Nd:YAG laser (Spitlight600, Innolas, Germany) as the light source, which emitted light at a wavelength of 266 nm. A micro-Raman system located in Renishaw, UK, equipped with a peltier-cooled charge-coupled device (CCD) detector and a 1800 lines/mm grating, was used to perform Raman scattering experiments. The selected excitation source was an Ar+ laser functioning at 514.5 nm. The spectrometer, intended to direct laser light onto the sample, was linked to an Olympus microscope (Model: MX50 A/T). The GRAM-32 program was used to aid in data collection. A fast-fast coincidence system using two 1-inch tapered BaF2 scintillators connected to XP 2020Q photomultiplier tubes was employed to measure the positron annihilation lifetime (PAL).

3. Results and discussion

3.1. XRD analysis

The XRD spectra for synthesized ZnO powder for different calcination temperatures are plotted in Fig. 1. At a reduced calcination temperature of 80 °C, zinc hydroxide nitrate hydrate (Zn5(OH)8(NO3)2(H2O)2) phase was observed. Increment in calcination temperature, pure ZnO with wurtzite phase becomes noticeable in the XRD patterns of the generated samples. The diffraction features linked to the (100), (002), (101), (102), (110), and (103) planes of the ZnO wurtzite structure (see JCPDS file no. 36-1451) align closely with the observed peaks. The diffraction pattern at higher calcination temperatures did not reveal any clear peaks associated with intermediate or secondary phases like Zn5(OH)8(NO3)2(H2O)2 or ε-Zn(OH)2. Consequently, at elevated calcination temperatures, all intermediate phases completely convert into crystalline ZnO.

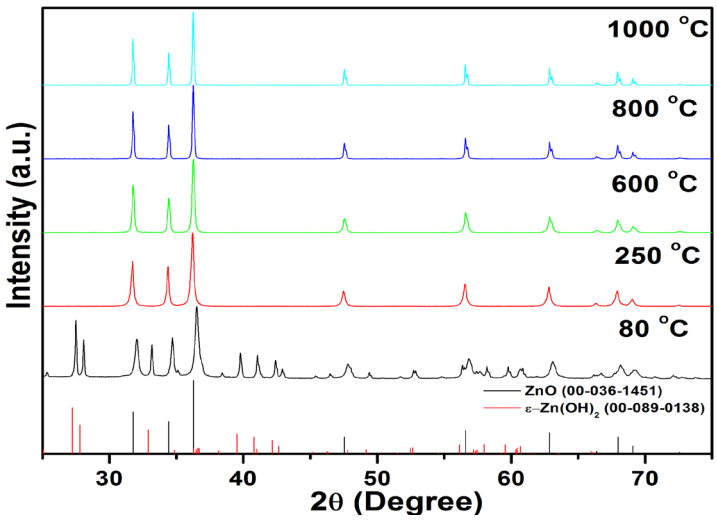

Fig. 1. XRD spectra for ZnO nanopowder with variation of calcinations temperature.

3.2. Raman spectroscopic analysis

The Raman scattering method is employed as a quick, sensitive, and non-invasive approach to examine crystallization, structural disorder within the lattice, and defects in micro-/nanostructures. Measurements are conducted at room temperature (RT) over a range of 200 to 1300 cm-1 utilizing an Ar+ laser. The Raman spectra of ZnO powder after being heat-treated at varying temperatures are presented in Fig. 2 (a-j). The Raman spectrum for ZnO powder heated to 80 °C is displayed in Fig. 2(a and f). In the lower frequency range of 200–800 cm−1, extra peaks can emerge because of different multiphonon modes (MP). Additional peaks linked to the intermediate phase of Zn may result from the creation of Zn5(OH)8(NO3)2(H2O)2 and residual nitrate precursor in the (NO3)2(H2O)2. With rising calcination temperatures, the intensities of these additional peaks typically diminish due to the improved crystallinity of the samples, a finding further corroborated by the XRD analysis.

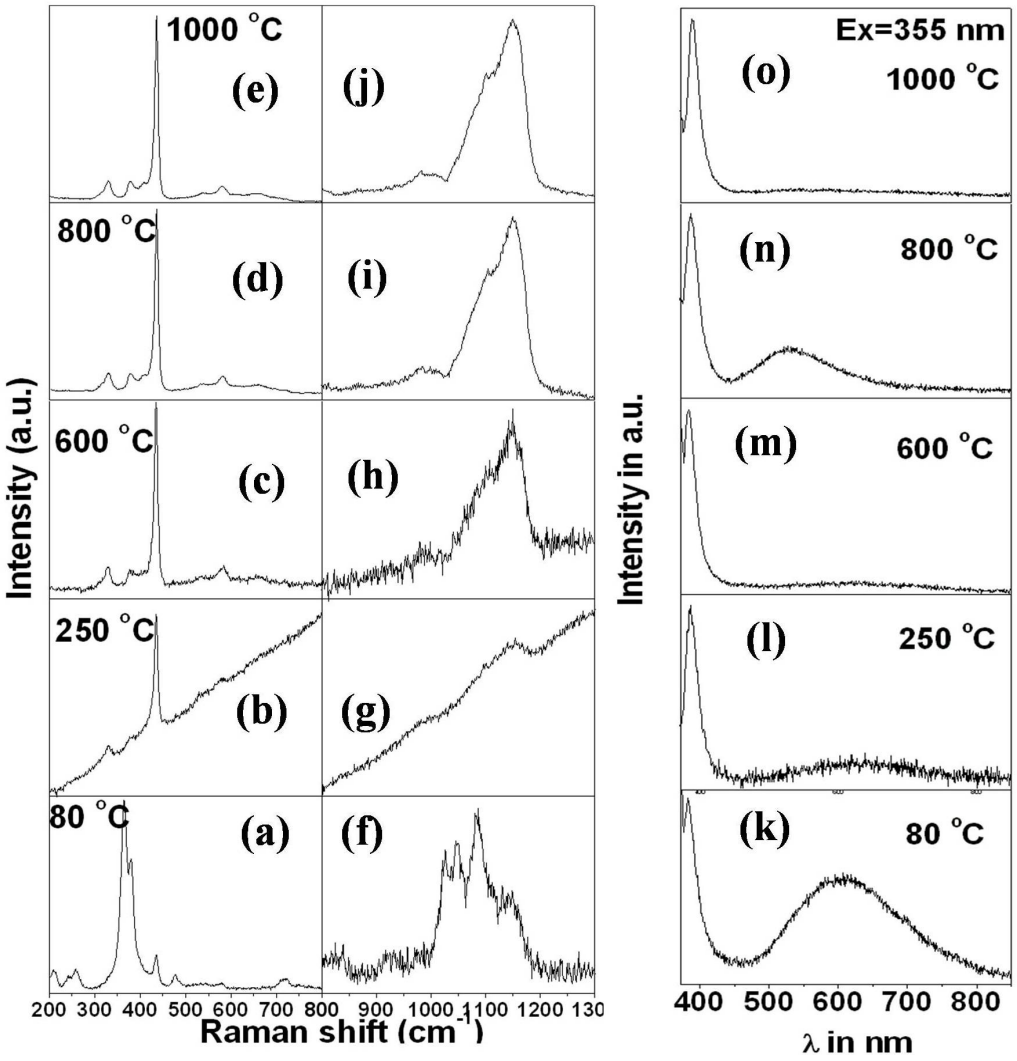

Fig. 2.The Raman spectrum (a, b, c, d, f, g, h, i, j); Photoluminescence spectrum (k, l. m, n, o) of synthesized ZnO powder with different calcination temperature.

In large wave number from 800 to 1300 cm−1, a broad Raman feature is identified at approximately 1053 cm−1 in the sample calcined at 80 °C. The features noted at 708 and 728 cm−1 are associated with in-plane deformation or zinc (Zn), oxygen vacancies (VO), defect clusters, and the bending (ν4) of the NO_3− ion. The existing intact NO_3− defects are relatively larger, leading to modes like symmetric stretching (ν1), out-of-plane deformation (ν2), asymmetric stretching (ν3), and in-plane deformation or bending (ν4). Both ν3 and ν4 modes show activity in both Raman and IR, whereas ν1 is active in Raman and ν2 is active in IR. With rising calcination temperatures, a wide band emerges in the range of 950 to 1200 cm−1, displaying considerable intensity. This wide band could include Raman modes linked to multi-phonon along with wulfenite secondary phase. The Raman modes at the elevated calcination temperatures were consistent with pure phase of ZnO, and no clear peaks showing any transitional/secondary phase.

3.3. Photoluminescence analysis

Fig. 2 (k-o) depicts photoluminescence spectra performed at room temperature of synthesized ZnO for variant calcinations temperature. It is observed that two bands are appeared in the all spectra with the varied intensity. The higher intensity at lower wavelength band is expected to be known as near band edge (NBE) transition. Another band with lower intensity at larger wavelength belongs to emission from deep band. The lower wavelength (~355 nm) is regarded as

free excitons recombination. Broad visible emission band is expected to arise due to many intrinsic defects related to vacancies, interstitial and group of vacancies. Form fig. 2 (k-m), intensity of visible broad band observed to be decrease with the increase in calcinations temperature from 80 °C to 600 °C because of relaxation of different responsible defects and vacancies. It has to be noticed at 800 °C calcined temperature that increment in the visible band intensity is found to be increase due to rise in Zn vacancy and their complexes. Therefore, temperature around 800 °C might be considered as a responsible temperature for generating the Zn vacancy. However, this broad visible band found suppressed for the sample calcined at 1000 °C due to retaining the stoichiometric situation in ZnO lattices. To explain this uncertainty in the luminescence behavior, the spectra is deconvoluted in fig. 3 (a&b) with best fitting of the experimental data for 80 °C &250 °C respectively. Following deconvolution, it becomes clear that visible broadband consists of a blend of green, yellow, orange, and red emissions. Because of the powder form of the samples, NBE emission peak intensity is used to normalize the data in place of the absolute PL intensity. Furthermore, this observable broadband intensity has been noted to diminish with rising calcination temperatures due to the relaxation of potential intermediate defect states associated with oxygen and its complexes.

Hence it can be predicted that stoichiometric ratio of ZnO can be increase with the increase in calcinations temperature. It can be understood that the quality/stoichiometric ratio of ZnO crystal is surely linked to the post heat treatment process, which can be used effectively to tune UV versus visible emission. Furthermore, PL spectra of calcined samples at 80 ºC & 1000 ºC provided an extra insight for defects/vacancies tuning in the ZnO crystal. These results indicate that the reappearance of DBE in 800 ºC calcined sample might be due do the depassivation of vacancies as all the hydrogen departed the lattice and forming complexes.

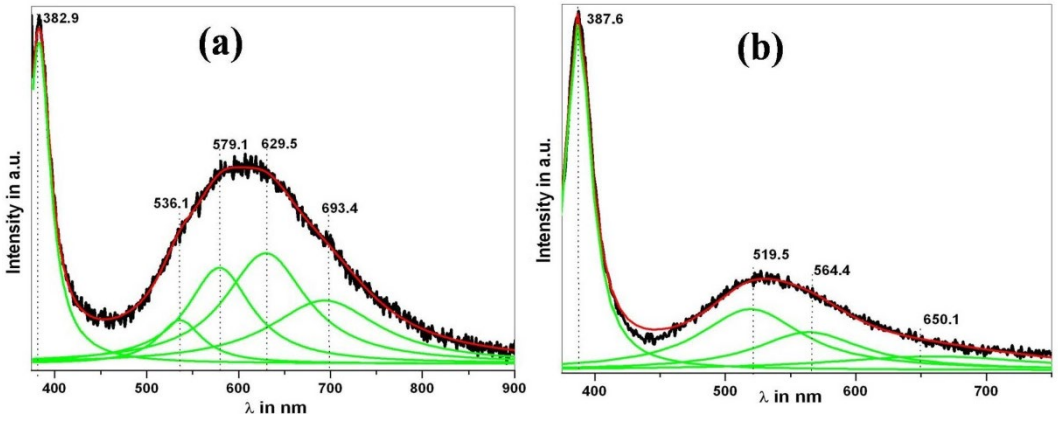

Fig. 3. Deconvolution of photoluminescence spectrum (a) 80 ºC; (b) 250 ºC.

3.4. XPS analysis

To comprehend the chemical bonding arrangement in ZnO nanopowders, XPS data were analysed for the samples calcined at various temperatures (80 ºC, 250 ºC& 1000 ºC). Fig. 4 (a, b & C) illustrates the deconvolution of wide oxygen O1s peaks for ZnO nanopowders. It is noticed that the O 1s peak shows highly asymmetric nature towards the higher binding energies, which can be considered as existence of different kind of oxygen impurities/vacancies and their complexes. The O 1s peak is deconvoluted in the form of three components (530.1 eV, 531.1 eV & 532.05 eV). Peak around 530.1 eVis expected to represent metal and oxygen (Zn-O) bond. Peak around 531.1 eV & 532.05 eV belong to oxygen deficiency (V_O) and interstitial oxygen (O_i) as well as species (CO_3, H_2O or O_2) chemisorbed on the surface of the ZnO nanopowders. It is observed that the area under peaks centered at 531.1 eV and 532.05 eV are found decreased with the increase in calcination temperature as depicted in fig. 4 (a, b& c) due to reduction in oxygen related vacancy/defects.

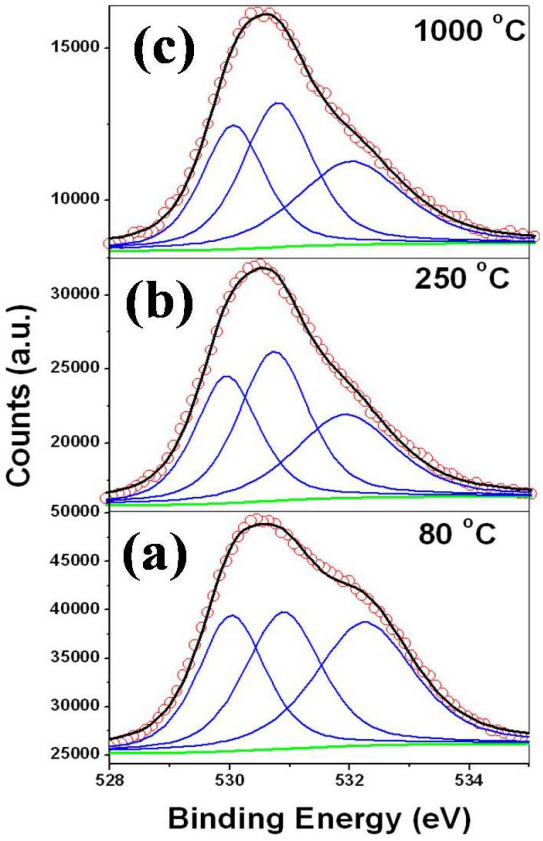

Fig. 4. O1s peak for ZnO nanopowders for different calcination temperature.

3.5. Positron annihilation analysis

To study the cationic defects, positron annihilation spectroscopy is performed for the samples calcined at different temperatures. Based on the characteristic of unmatched life time of positron trapped in different defects is utilized to examine different kind of defects/voids/impurities/complexes. Fig. 5(a) shows the positron annihilation lifetime spectra for the samples calcined at different temperatures. Table 1 details the three lifespan elements that most closely correlate with the spectra: τ1, τ2, and τ3. The briefest lifetime component, τ1, related to intensity I1, corresponds to positron annihilation taking place at structural defects located within the grain boundaries. In a bulk material, τ1 indicates positron annihilation in defect-free areas, where clearly defined grain boundaries act as essential trapping locations. The intermediate lifetime, τ2, with intensity I2, signifies the positron annihilation occurring at the nanovoids located at the triple junctions. The major part of the positron lifetime, τ3, associated with intensity I3, is connected to the pick-off annihilation of ortho positronium created in the sizable intercrystalline regions.

It has to be noticed here that positron annihilation with the presence of Zn vacancies is a common phenomenon in ZnO. Fig. 5 (b) shows the positron life time variation in the samples against calcination temperatures. Life time τ_1& $\tau_2$are observed to be decreased with the increase in calcination temperatures as expected due to the decrement in the different defects/vacancies/voids. This result is well matched with the outcome of PL and XPS measurements. Table 1 shows the all life time components and related intensities to provide a comparative insight for the all samples. This increased $\tau_3$annihilation life time in samples is related to V_{Zn} and expected to decrease through complex formation with hydrogen,V_{Zn}-H.Some uncommon di-vacancies (V_{Zn+O}) also controls the life time of positron annihilation, which is expected to decrease. In our case, lower life time at higher calcination temperature is well matched within the range of life time of positron annihilation corresponding to the cluster of Zn and O di-vacancies. However, the larger annihilation life time with lower calcinations temperatures are due to the cluster of di-vacancies

and the secondary phase of $Zn(OH)_2$. Therefore, increased calcinations time is expected to reduce the vacancies clusters and secondary phases, which is matched with the above characterizations. Another aspect related to complex formation of Zn vacancy with hydrogen also confirmed.

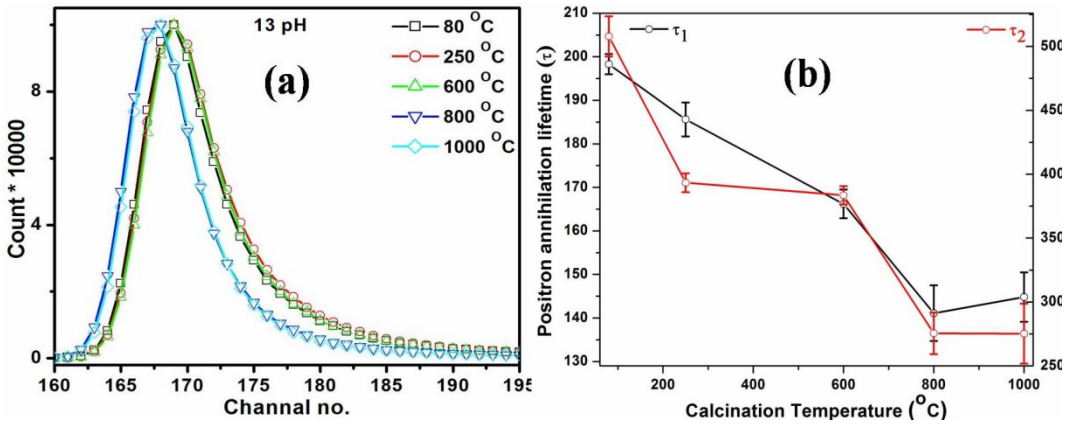

Fig. 5.(a) Positron lifetime spectrum; (b) Variation of life.

Table 1. Positron annihilation lifetimes (τ) and corresponding intensities (I) of ZnO nanopowders calcined at different temperatures.

ZnO 13 pH temperature	Positron Lifetime (ps)			Defect Relative Intensities		
	τ_1	τ_2	τ_3	I_1	I_2	I_3
Raw	198.3±2.3	507.9±15.7	2161.2±97.6	76.05±1.24	22.01±14	1.94±.15
250	185.6±3.9	393.3±7.4	3936.6±131.7	58.10±2.17	40.58±2.15	1.31±.05
600	166.2±3.3	383.5±7.2	2267.5±258.9	59.19±1.8	40.32±1.77	.48±.09
800	141.1±6.4	275.5±16.3	1021.9±100.7	60.01±6.11	37.98±5.8	2.01±.41
1000	144.8±5.7	275.2±23.5	983.7±160.1	70.8±6.71	27.94±6.38	1.26±.44
τ_1, τ_2, and τ_3 are Positron Life Time with Relative Intensities I_1, I_2, and I_3						

4. Conclusion

An easy and fast synthesis route for ZnO nanoparticles has been presented in this paper for tuning of hydrogen impurity with the tuning of calcination temperature. Hydrogen impurity was discussed through the formation of complexes with Zn vacancy. This synthesis route was found promising for the co-existence of Zn vacancy and Hydrogen impurity. Further, di-vacancies of Zn and O also discovered and argued in the synthesized ZnO nanoparticles. Results were supported with different characterization techniques such as XRD, photoluminescence, Raman spectroscopy and positron annihilation analysis. Variation of different intermediate phases and broad luminescence in visible region from low to high temperature calcination provided a good leap of clarity with many defects/vacancies and their complexes. Analysis of positron life time components was found very effective and conclusive to decide the role of different defects and vacancies with respect to different calcination temperatures.

References

[1] Singh, V.P; Das, D.; Rath, C., Materials Research Bulletin 48, 682-686 (2013); https://doi.org/10.1016/j.materresbull.2012.11.026

[2] Singh, V.P.; Kumar, M.; Reddy, B.P.; Sunny, Gangwar, R.K., Rath, C., Crystals 10, 1025

(2020); https://doi.org/10.3390/cryst10111025

[3]Xu, W.L.; Zheng, M.J.; Ding, G.Q.; Shen, W.Z. Chem. Phys. Lett. 411, 37-42 (2005); https://doi.org/10.1016/j.cplett.2005.05.105

[4] Huang, M.H.; Mao, S.; Feick, H.; Yan, H.; Wu, Y.; Kind, H.; Weber, E.; Russo, R.; Yang, P., Science 292, 1897-1899 (2001); https://doi.org/10.1126/science.1060367

[5] Guo, L.; Ji, Y.L.; Xu, H.; Simon, P.; Wu, Z., J. Am. Chem. Soc. 124, 14864-14865 (2002); https://doi.org/10.1021/ja027947g

[6] Pan, Z.W.; Dai, Z.R.; Wang, Z.L. Science 291, 1947-1949 (2001); https://doi.org/10.1126/science.1058120

[7] Kong, X.Y.; Ding, Y.; Yang, R.; Wang, Z.L., Science 303, 1348-1351 (2004); https://doi.org/10.1126/science.1092356

[8] Zhang, J.; Sun, L.; Liao, C.; Yan, C., Chem. Commun. 3, 262-263 (2002); https://doi.org/10.1039/b108863g

[9] Fan, H.J.; Scholz, R.; Kolb, F.M.; Zacharias, M.; Gösele, Solid State Commun. 130, 517-521 (2004); https://doi.org/10.1016/j.ssc.2004.03.014

[10] Lao, J.Y.; Wen, J.G.; Ren, Z.F. Nano Lett. 2, 1287-1291 (2002); https://doi.org/10.1021/nl025753t

[11] Kim, K.-S.; Kim, H.W. Phys. B Condens. Matter 328, 368-371 (2003); https://doi.org/10.1016/S0921-4526(02)01954-3

[12] Kumar, M.; Dubey, S.; Rajendar, V.; Park, S.H., Journal of Electronic Materials 46, 6029-6037, (2017); https://doi.org/10.1007/s11664-017-5565-y